Procedia Computer Science

Volume 80, 2016, Pages 1392–1403

ICCS 2016. The International Conference on Computational Science

Localized computation of Newton updates in fully-implicit two-phase flow simulation

Soham M. Sheth and Rami M. Younis

The University of Tulsa, Tulsa, Oklahoma, USA
soham-sheth@utulsa.edu, rami-younis@utulsa.edu

Abstract

Fully-Implicit (FI) Methods are often employed in the numerical simulation of large-scale subsurface flows in porous media. At each implicit time step, a Newton-like method is used to solve the FI discrete nonlinear algebraic system. The linear solution process for the Newton updates is the computational workhorse of FI simulations. Empirical observations suggest that the computed Newton updates during FI simulations of multiphase flow are often sparse. Moreover, the level of sparsity observed can vary dramatically from iteration to the next, and across time steps. In several large scale applications, it was reported that the level of sparsity in the Newton update can be as large as 99%. This work develops a localization algorithm that conservatively predetermines the sparsity pattern of the Newton update. Subsequently, only the flagged nonzero components of the system need be solved. The localization algorithm is developed for general FI models of two phase flow. Large scale simulation results of benchmark reservoir models show a 10 to 100 fold reduction in computational cost for homogeneous problems, and a 4 to 10 fold reduction for strongly heterogeneous problems.

Keywords: Fully-Implicit, Localization, Newton's Method, and porous media

1 Introduction

Numerous physical phenomena are modeled using nonlinear and variable-coefficient forms of the Advection-Diffusion-Reaction (ADR) partial differential equations (PDEs) [3]. These include geologic subsurface multiphase flows [1, 6, 8, 2], large-scale and steady fluid dynamics [5, 7] and atmospheric flows [11, 4]. These phenomena are generally characterized by a stiff nonlinear coupling and a wide disparity in the range of varying coefficients. Furthermore, in many applications there is a need to model large-scale domains while capturing critical, intrinsically local effects. As a consequence of these factors, modern numerical methods must somehow balance robustness with computational efficiency.

For the class of problems at hand, implicit numerical approximations are particularly attractive owing to their unconditional stability with respect to the time-step size (see for example [1, 2]). An implicit time-step requires the solution of a tightly coupled nonlinear system of

 Selection and peer-review under responsibility of the Scientific Programme Committee of ICCS 2016

doi:10.1016/j.procs.2016.05.445

discrete residual equations given the target time-step size and the initial state vector for the time-step. An often cited limitation of implicit methods remains to be their need for the solution of large coupled nonlinear algebraic systems at each time step. Due to the nonlinear nature of the governing equations, Newton-like iterative processes are the method of choice, and subsequently, requires the solution of a large linear system at every iteration.

Recent mathematical developments show that there is significant locality present with the Newton updates. [12, 9] present a novel algorithm to characterize this locality and reduce the size of the linear system which increases the computational efficiency. [10] applies this algorithm to two phase sequential implicit simulation of flow and transport.

This work extends the solution strategy to three-dimensional two-phase fully implicit simulation. This is a meaningful point of departure for the development of adaptive solution methods for more general problems.

2 General approach

Fluid flow in porous media can be described by the canonical equation

$$\partial_t a(u) + \partial_x f(u) + \partial_x G(u, \partial_x u) + s(u) = 0, \quad \text{in } (0,T)\times\Omega, \tag{1a}$$

$$\alpha(u) + \beta\left(\frac{\partial u}{\partial \nu}\right) = w, \quad \text{in } (0,T)\times\partial\Omega, \tag{1b}$$

$$u = u_0, \quad \text{for } t = 0 \text{ and } x \in \partial\Omega \tag{1c}$$

where Ω is a bounded domain in $\mathbb{R}^d$ with boundary $\partial\Omega$ and $(d = 1, 2, 3)$; $\frac{\partial u}{\partial \nu}$ denoted the gradient along the outward oriented unit-normal on $\partial\Omega$; $u = (u_1, \ldots, u_m)^T$ is the state vector that is comprised of the independent state variables, $u_i : \Omega \times (0,T) \to \mathbb{R}$, for $i = 1, \ldots, m$; $a(u)$ is the accumulation; $f(u)$ is the inviscid flux; $G(u, \partial_x u)$ is the viscous flux, and $s(u)$ are the reaction terms.

Upon the semi-discretization in time, the independent state vector $u^{n+1} = (u_1^{n+1}), \ldots, u_m^{n+1}{}^T$ is introduced, where $u_i^{n+1} : \Omega \to \mathbb{R}$, $i = 1, \ldots, m$. The solution, u^{n+1}, is the approximation to the independent state vector at discrete time level $n+1$; i.e., $u^{n+1}(x) \approx u(x, t^{n+1})$. The type of implicit discretization is unimportant so long as the resulting semi-discrete form has a single stage. Linear multistep methods follow this paradigm for example. In what follows we drop the superscript indicating the discrete time level, and we assume that all variables are at the $n+1$ level. The corresponding canonical form of the semi-discrete equations becomes,

$$R_\infty(u) := s(u) + \partial_x f(u) + \partial_x G(u, \partial_x u) = 0, \quad \text{in } \Omega, \tag{2a}$$

$$B_\infty(u) := \alpha u + \beta \frac{\partial u}{\partial \nu} = w, \quad \text{in } \partial\Omega, \tag{2b}$$

where $s(u)$ incorporates both the reaction and discrete accumulation. The dependence on the approximations at previous time levels is implied by the fact that all terms in Equations 2 are spatially variable. Equation 2 is a nonlinear system of PDE and is referred to as the *infinite-dimensional problem*.

Assuming Fréchet differentiability (denoted by R'_∞), and invertability of the derivative, Newton's method may be applied to solve Equation 2. Given an initial guess, u^0, the infinite-dimensional Newton updates,

$$\delta_\infty^\nu(x) := u^{\nu+1} - u^\nu, \quad \nu = 1, \ldots,$$

are obtained by solving the linear PDE,

$$R'_\infty(u^\nu)\delta^\nu_\infty + R_\infty(u^\nu) = 0, \quad \text{in } \Omega, \tag{3a}$$

$$\alpha\delta^\nu_\infty + \beta\frac{\partial}{\partial\nu}\delta^\nu_\infty = 0, \quad \text{in } \partial\Omega, \tag{3b}$$

Analogously, assuming that the finite-dimensional residual equations are differentiable, and that the resulting Jacobian matrix is invertible, the finite-dimensional problem may be solved using Newton's method as well. The iteration is started from U^0_h, and the update directions are obtained by solving the linear algebraic system,

$$R'_h(U^\nu_h)(\delta^\nu_h) + R_h(U^\nu_h) = 0 \;\; \nu = 1, \ldots. \tag{4}$$

The infinite- and finite-dimensional Newton iterates are also realed to each other through the spatial discretization error. This situation is summarized in Figure 1. Assuming a sufficiently

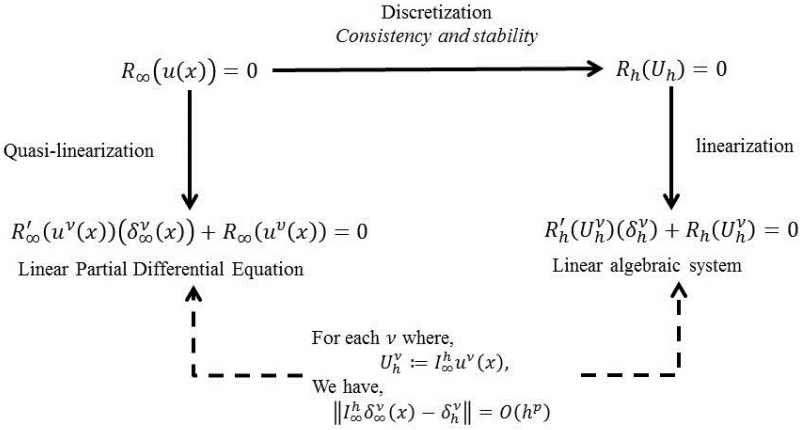

Figure 1: The connections between the Newton processes for the infinite- and finite-dimensional problems.

accurate discretization, and requiring the infinite norms, we have that the nonzero support of the infinite update is equation to that the numerical update,

$$\text{supp } \delta^\nu_\infty = \text{supp } \delta^\nu_h.$$

The approach taken in [12, 9, 10] is to seek an analytical approximation to the solution of the problem 3. An approximation is necessary as the problem has generally variable coefficients, and despite beng linear, the direct solution may be intractable. Nevertheless, the approximate solution, δ^*, is derived such that,

$$\|\delta^*\| \geq \|\delta_\infty\|, \tag{5}$$

thereby guaranteeing that the support of the estimate is conservative,

$$\text{supp } \delta^* \supseteq \text{supp } \delta^\nu_\infty \approx \text{supp } \delta_h.$$

In multiple dimensions, the analytical solution to the linear problem described above is challenging. Next, we present an algorithm that produces conservative estimates.

3 Fully implicit multidimensional algorithm

The infinite-dimensional Newton iteration is a linear Partial Differential Equation (PDE) with variable coefficients. For flow, Equation 3 becomes the screened Poisson equation (or the modified Helmholtz equation), and for transport, it reduces to a first-order hyperbolic equation with no time component. Since the PDEs are linear, superposition may be applied by the decomposition of the residual into a serious of bump functions, each of which has a disjoint and compact support. This allows us to derive the estimate that is composed of the sum of the solutions of each sub-domain. In order to use the superposition principle efficiently, for each compactly supported residual component, the PDE may be solved analytically. In multiple dimensions, closed form analytical solutions for general variable coefficient PDEs are almost impossible to obtain. Following the procedure described in [10], instead of seeking exact analytical update, δ_∞, we may choose to solve a similar but simpler problem for a conservative estimate, δ^*, that satisfies condition given in Equation 5.

Similar to the algorithm developed in [10], we will seek spherically symmetric solutions that will be conservative to the solutions obtained within a three-dimensional cubic space. For highly heterogeneous problems, the solutions obtained will be overly conservative due to the strong spatial correlation in the variable coefficients of the Newton problem.

For coupled flow and transport, the infinite-dimensional Newton iteration is a system of linear PDEs. If $R_p(p,s)$ and $R_s(p,s)$ represent the governing equations for flow and transport, respectively, then the Newton iteration is given by

$$\begin{bmatrix} \frac{\partial R_p(p+\epsilon\delta_p,s)}{\partial\epsilon}\Big|_{\epsilon=0} & \frac{\partial R_p(p,s+\epsilon\delta_s)}{\partial\epsilon}\Big|_{\epsilon=0} \\ \frac{\partial R_s(p+\epsilon\delta_p,s)}{\partial\epsilon}\Big|_{\epsilon=0} & \frac{\partial R_s(p,s+\epsilon\delta_s)}{\partial\epsilon}\Big|_{\epsilon=0} \end{bmatrix} = -\begin{bmatrix} R_p(p,s) \\ R_s(p,s) \end{bmatrix}, \tag{6}$$

where $\frac{\partial R_u(u+\epsilon\delta_u,v)}{\partial\epsilon}\Big|_{\epsilon=0}$ is the Fréchet derivative, which evaluates to $\frac{\partial R_u(u,v)}{\partial u}\cdot\delta_u$. We postulate that a conservative estimate, δ^*, can be obtained by neglecting the off-diagonal entries in the matrix system given by Equation 6 and solving a decoupled system for flow and transport.

With an analytical solution of Equation 3, the following algorithm can be used to identify the support of the discrete Newton update:

1. Inspect the discrete residual vector. If it is sparse, we proceed to step 2. Otherwise, the original system is solved.
2. For each nonzero residual entry:
   (a) Project the nonzero entry onto a piecewise constant bump function whose support is the corresponding grid cell.
   (b) Use the analytical estimate to obtain the radius of the anticipated support due to the residual entry; supp δ^*.
   (c) Flag all cells within the radius from the i-th cell.
3. Solve the discrete Newton system for the flagged cells only by removing the rows and columns of all unflagged cells from the Jacobian matrix.

The complexity of this algorithm scales linearly with the number of nonzero residual entries, $O(||R_h||_0)$. Next we derive the decoupled analytical estimates for flow and transport for three-dimensional problems, which corresponds to the solution of Equation 6 by neglecting the off-diagonal matrix entries. The equations derived will be used to obtain a *priori* estimates of the nonzero support of the Newton updates for a fully implicit time stepping algorithm.

4 Flow

The following second order differential equation describes fluid flow in porous media in multiple dimensions. The canonical form is give by

$$\frac{\partial a(p(x,t))}{\partial t} + \nabla(K(p(x,t),x)\nabla(p(x,t))) = w(p(x,t)), \quad \text{in } (0,T)\times\Omega, \tag{7}$$

with the auxiliary conditions

$$K(p,x)\nabla p = 0, \qquad \text{in } \partial D,\ t \geq 0, \tag{8a}$$

$$p = p^0, \qquad t = 0, \tag{8b}$$

where $K(u,x)$ is a nonlinear mobility function which incorporates spatially varying diffusion coefficient and a dynamic mobility dependency. In most applications K is solely a function of u but in cases with spatial heterogeneity, its a direct function of u and x. $a(u)$ is mostly nonlinear and it incorporates a heterogeneous porosity and general density dependencies. The net source term is denoted by $w(u)$ and it may be spatially and temporally variable. Equation 7 reduces to a reaction-diffusion equation when $K(u,x)$ is constant. The semi-discrete form of Equation 7 is

$$R_p(p^{n+1}) = a(p^{n+1}) - a(p^n) + \Delta_t\nabla.[K(p^{n+1},x)\nabla p^{n+1}] - w(p^{n+1}). \tag{9}$$

Subsequently, the infinite-dimensional Newton iteration becomes

$$\begin{aligned} R_p(p^\nu) &= -R_p'(p^\nu)\delta_p \\ &= -\left[\{a'(p^\nu) - \Delta_t w'(p^\nu)\}\delta_p + \Delta_t\nabla\{\nabla\left[K(p^\nu,x)\delta_p\right] - \nabla K(p^\nu,x)\delta_p\}\right]. \end{aligned}$$

Assuming no spatial variation in K i.e., $\nabla K(p,x) = 0$, the above equation reduces to

$$\Delta\hat{\delta}_p(x) + h(x)\hat{\delta}_p(x) = -R_p(x), \tag{10}$$

where $\hat{\delta}_p = \Delta_t K(p,x)\delta_p$ and

$$h(x) = \frac{a'(p) - \Delta_t w'(p)}{\Delta_t K(p)}.$$

As described in the previous section, instead of seeking solution of Equation 10, we solve a similar equation such that we obtain conservative solution. It is postulated that for a modified Helmholtz equation, the infimum of the variable coefficient, $h(x)$, produces the most conservative estimates. Using the infimum of the variable coefficients, the estimates obtained may sometimes be highly conservative. Through experiments, it was observed that harmonic mean averaging also provide conservative estimates and are less conservative than the estimates obtained by taking the infimum as the homogenization strategy. Therefore, letting

$$\lambda_{avg}^2 = -\text{harmmean}_{x\in\Omega}h(x),$$

we obtain

$$\Delta\delta_p^*(x) - \lambda_{avg}^2\delta_p^*(x) = -R_p(x). \tag{11}$$

For a two-dimensional problem, a step wise solution is obtain in [10]. Following the same method, we obtain spherically symmetric solutions of Equation 11. Assuming a nontrivial residual bump function, β, with a nonzero support of radius r_1,

$$\delta_p(r) = \frac{\beta e^{\lambda_{avg}(r_1-r)}}{2\lambda_{avg}\Delta_t K(p,r)}\left[\frac{R^2}{r(1+\lambda_{avg}R)} - \frac{1}{\lambda_{avg}}\right], \tag{12}$$

where, R is the domain boundary and Δ_t is the time step size. The radius of the nonzero support of the Newton update can be computed from the above expression numerically by equating the right hand side to machine precision number.

5 Transport

Transport equation governs the motion of a conserved scalar field as it is transported by a known velocity vector field. One such process is the flow of fluids in porous media described by the hyperbolic conservation laws. The canonical form of the saturation equation is given by

$$\frac{\partial a(s(x,t))}{\partial t} + \nabla \cdot f(s(x,t)) = w(s(x,t)), \quad \text{in } (0,T) \times \Omega, \tag{13}$$

where $f(s)$ is a general nonlinear flux function, $a(s)$ is the mass accumulation term and $w(s)$ is a source term. The auxiliary conditions prescribed here are

$$f(s(x,t)).\hat{n} = 0, \qquad \text{in } \partial D,\ t \geq 0, \tag{14a}$$

$$s = s^0, \qquad t = 0. \tag{14b}$$

The semi-discrete form of Equation 13 is

$$R_s(s^{n+1}) := a(s^{n+1}) - a(s^n) + \Delta_t \nabla \cdot f(s^{n+1}) - \Delta_t w(s^{n+1}), \tag{15}$$

where Δ_t is the time step size. Following the procedure described in the previous sections, the Fréchet derivative results in a *quasilinear* differential equation given by

$$R'_s(s^{n+1})\delta_s := \{a'(s^{n+1}) - \Delta_t w'(s^{n+1})\}\delta_s + \Delta_t \nabla \cdot (f'(s^{n+1})\delta_s). \tag{16}$$

Subsequently, the infinite-dimensional Newton iteration becomes

$$\begin{aligned} R_s(s^\nu) &= -R'_s(s^\nu)\delta_s \\ &= -\left[\{a'(s^\nu) - \Delta_t w'(s^\nu)\}\delta_s + \Delta_t \nabla \cdot (f'(s^\nu)\delta_s)\right]. \end{aligned}$$

The above equation reduces to

$$\nabla \hat{\delta}_s(x) + h(x)\hat{\delta}_s(x) = -R_s(x), \tag{17}$$

where $\hat{\delta}_s = \Delta_t f'(s)\delta_s$ and

$$h(x) = \frac{a'(s) + \Delta_t w'(s)}{\Delta_t f'(s)}.$$

The solution obtained in [10] for a two-dimensional case decomposes the residual function into summation of several bump functions. Following the same procedure, the solution in three-dimensions is

$$\delta_s(r) = \frac{\delta_s^*(r^*)}{\Delta_t f'(s)} \frac{r^{*2}}{r^2} e^{-\lambda_{min}(r-r^*)}, \tag{18}$$

where r^* is the position of the residual, δ^* is the Newton update experienced by the gridcell contained within r^* and λ_{min} is the infimum over all $h(x)$.

From Equation 18, the radius of the nonzero support of the Newton update caused by the residual at r^* is computed by

$$\begin{aligned} r &= \frac{2}{A} W_n \left(\frac{A}{2\sqrt{B}} \right) \\ &= \frac{2}{A} \left[log\left(\frac{A}{2\sqrt{B}} \right) - log\left(log\left(\frac{A}{2\sqrt{B}} \right) \right) - log\left(1 - \frac{log\left(log\left(\frac{A}{2\sqrt{B}} \right) \right)}{log\left(\frac{A}{2\sqrt{B}} \right)} \right) \right], \end{aligned}$$

where $W_n(x)$ is the Lambert function evaluated at x, $A = \lambda_{min}$ and $B = \frac{\epsilon_m \Delta_t f'(s)}{\delta_s^*(r^*) r^* exp[\lambda_{min} r^*]}$.

6 Results

Incorporating the analytical estimates derived in the previous sections in a two phase reservoir simulator, we estimate the radius of influence for each nonzero residual entry. The union of all the sub-domains that result from individual flagging, forms the new and reduces computational domain for the linear solver. The first test case is a homogeneous permeability field with $1,122,000$ gridcells (60X220X85). One production and one injection well act as a source and a sink with slight compressibility in the problem. Figure 2 shows the simulation results for a few time steps with the time-step size increasing stepwise, shown by the green curve on the secondary axis. The primary y-axis is the percentage of domain that is solved every iteration. For conventional solution strategies, the entire domain is solved every iteration, resulting in a straight line at 100% as its ordinate. The red curve in Figure 2 is the actual domain that is showing a nonzero Newton update or in other words active. The rest of the domain, which is inactive, if excluded from the computational domain will neither affect the solution nor degrade the nonlinear convergence rate. The blue curve is an *a priori* estimate of the active domain obtained by applying the aforementioned algorithm. As it can be observed, the estimate is consistently conservative to the *a posteriori* numerical solution. The maximum domain that needs to be solved is around 25%, with an average of 8.5%.

The corresponding increase in the computational efficiency is shown by computing the complexity of the new algorithm against that of the conventional methods. Suppose that the computational cost for a linear solver is given by

$$cost = \alpha N^{\beta}, \tag{19}$$

where N is the size of the problem, α and β are constants. Usually, the values of β for a linear solver range from $1.1 - 1.5$. In Table 1 the first row gives the increasing values of β, second row shows the ratio of the complexity of the developed localized algorithm to that of the conventional full field simulation, give by

$$ratio = \frac{\alpha \sum_{i=1}^{n} (\%N_i)^{\beta}}{\alpha n N^{\beta}},$$

where n is the total number of iterations and $\%N_i$ is the reduced size of the domain as predicted by the algorithm. The folds increase in the computational efficiency is given in the third row. For an average β value of 1.4, the localized algorithm will be 28 times faster compared to solving the entire domain every iteration. Stronger the locality, higher will be the computational gains.

The second test case is the highly heterogeneous SPE10 comparative study with $1,122,000$ gridcells (60X220X85), shown in Figure 3. Due to a huge contrast in the values of the variable

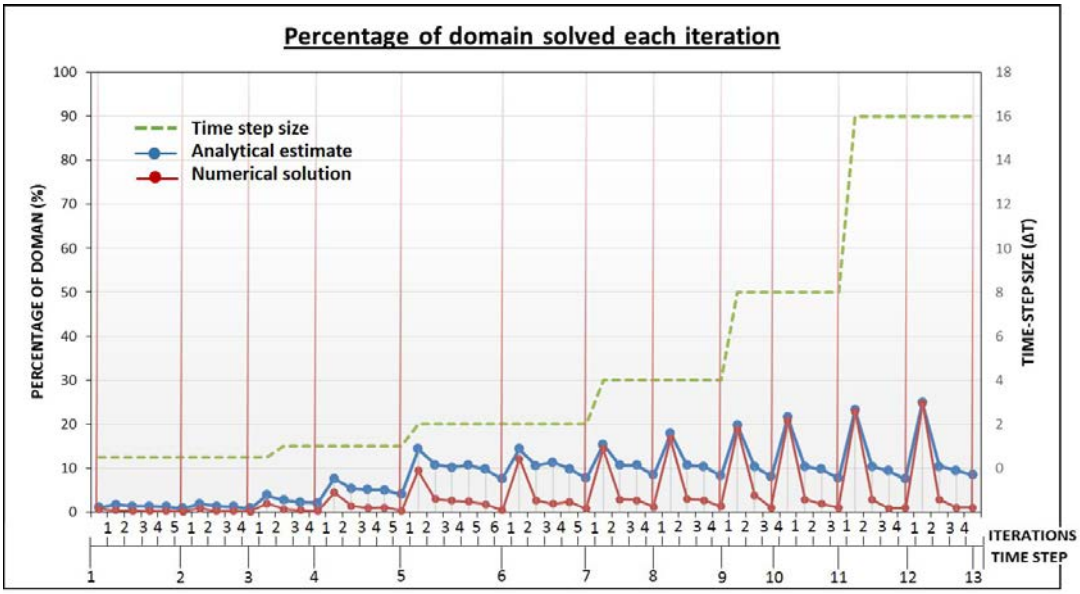

Figure 2: Percentage of domain solved over several time-steps for a homogeneous permeability field.

coefficient, the homogenization of the pressure equation leads to overly conservative estimates. Saturation equation being hyperbolic in nature results in highly local estimates.

Table 1: Complexity analysis for localized linear solver for a homogeneous domain.

β value	1.0	1.2	1.4	1.6	1.8	2.0
$\frac{\alpha \sum_{i=1}^{n} (\%N_i)^{\beta}}{\alpha n N^{\beta}}$	0.0847	0.0546	0.0356	0.0235	0.0156	0.0105
Folds faster	11.80	18.29	28.03	42.50	63.83	95.03

Table 2: Complexity analysis for localized linear solver for the SPE10 comparative study case (60X220X85 gridcells).

β value	1.0	1.1	1.2	1.3	1.4	1.5	1.6	1.7	1.8	1.9	2.0
$\frac{\alpha \sum_{i=1}^{n} (\%N_i)^{\beta}}{\alpha n N^{\beta}}$	0.38	0.34	0.32	0.29	0.27	0.24	0.22	0.21	0.19	0.17	0.16
Folds faster	2.65	2.90	3.16	3.45	3.76	4.10	4.46	4.86	5.30	5.77	6.28

Stricter estimates can be obtained by devising alternate strategies for homogenizing the variable coefficient equation. One such strategy is shown in the next section. Observing the nonzero Newton updates for pressure and saturation over several iterations, see Figure 4, show that there is no uniform trend visible, thus rendering ad hoc prediction methods unreliable. In Figure 4, blue shaded area is obtained by the application of the algorithm described in this paper while the green shaded area is the result from the numerical simulator. As it can be easily observed, the new algorithm is conservative and sharp at all points in the domain, thus

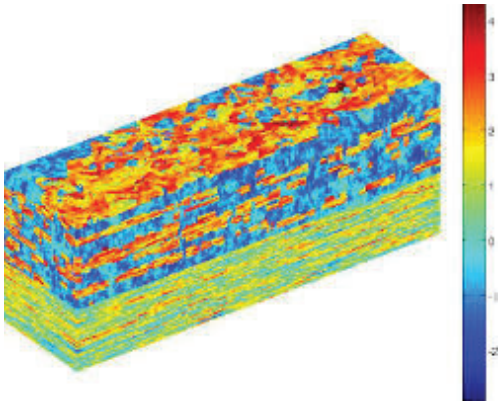

(a) Logarithm of permeability in the x-direction for the full SPE10 case.

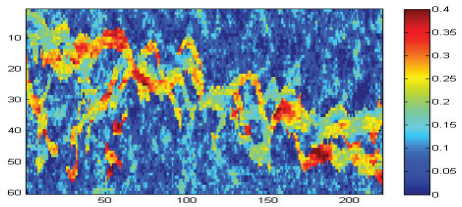

(b) Logarithm of permeability for the 48th layer of SPE10.

Figure 3: SPE 10 comparative geological model permeability field.

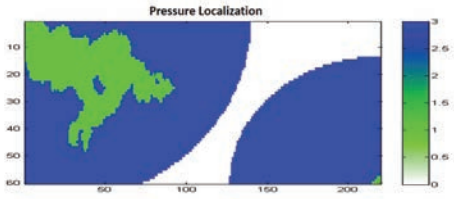

(a) Iteration 1: Pressure

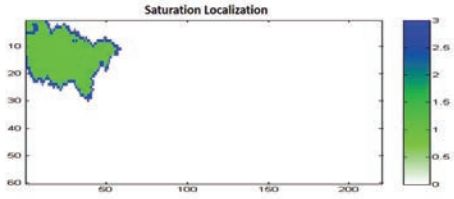

(d) Iteration 1: Saturation

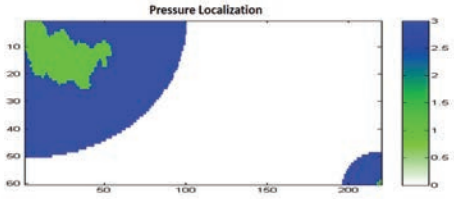

(b) Iteration 2: Pressure

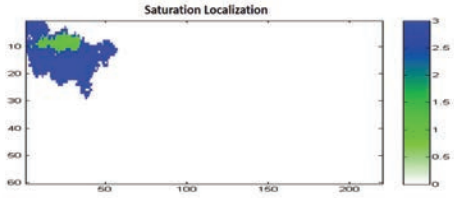

(e) Iteration 2: Saturation

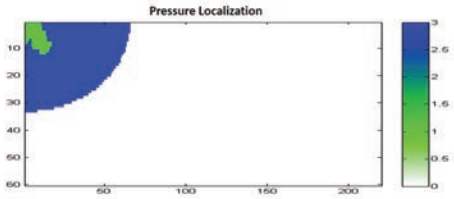

(c) Iteration 3: Pressure

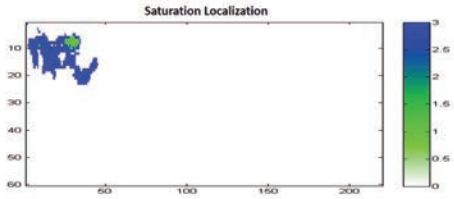

(f) Iteration 3: Saturation

Figure 4: Nonzero Newton updates for pressure and saturation over three consecutive iterations. The blue shaded ares is obtained by using the algorithm described in the paper while the green area is the actual domain showing a nonzero Newton update. Our estimates are conservative and sharp.

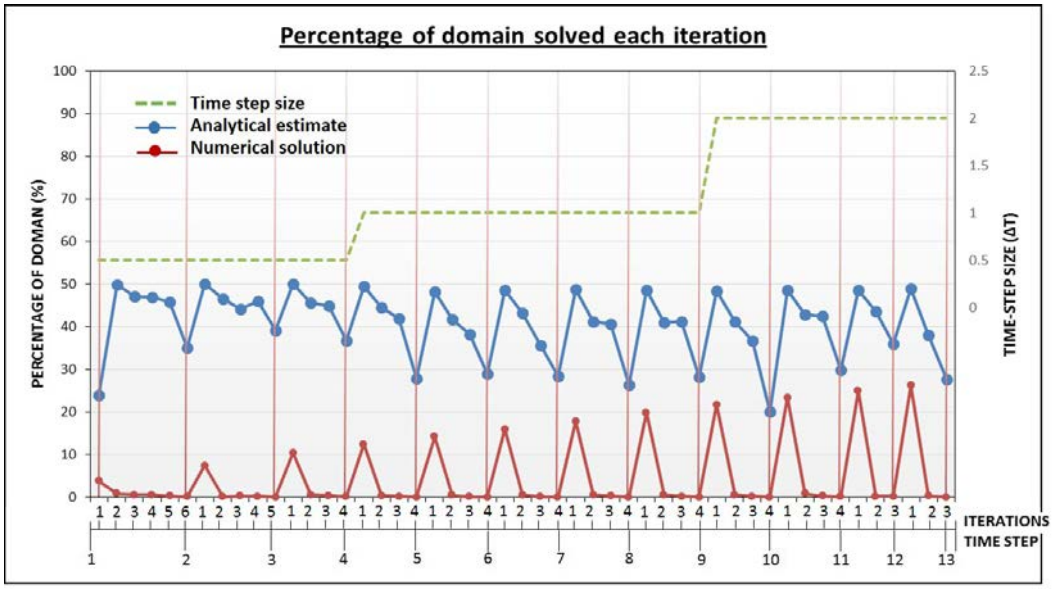

Figure 5: Percentage of domain solved over several time-steps for the SPE10 comparative study case.

proving to be a reliable method for the prediction of locality present in the nonlinear solution process. Another important observation made is that the degree of locality increases over iterations. From Figure 5 it can be observed that the first iteration for pressure result in a fairly global update but the subsequent iterations are all local. The overall computational gains are summarized in Table 2.

Depending on the complexity of the linear solver, the localized algorithm will result in improved computational speed. The average gain in the computational efficiency is around 4 folds. Even for the worst case scenario, this algorithm is 2.6 times faster than the full field solution strategies. The higher gains are a result of the strictly localized behavior of the hyperbolic equation. With multicomponent systems, the gains would be substantially higher than two phase simulations.

7 Homogenization strategy

The homogenization strategy that result in conservative estimates theoretically is the infimum strategy. In other words, taking the infimum of the variable coefficient on the domain results in a constant coefficient second order equation whose solution is always conservative to the solution of the variable coefficient equation. Through experiments, it was observed that this strategy can be replaced by harmonic mean averaging. In this section we present an alternate strategy that result in very sharp estimates that might not be conservative at all times. It was also observed that even though the estimates are not conservative in some cases, the nonlinear convergence rate is not affected. Figure 6 is obtained by simulating the first 20 layers layers of the SPE10 comparative study case for several time-steps. It can be readily seen that the arithmetic averaging strategy result if very sharp estimates as the difference between the blue and the red curves is significantly smaller than the one for harmonic averaging

strategy in Figure 5. Sharp estimates mean high computational gains. Hence, using arithmetic averaging instead of harmonic averaging will result in higher computational gains at the expense of nonconservative estimates. For this case, the estimates obtained are always conservative, which might not be the case in more complex cases. Further investigation is required to develop conservative and sharp homogenization strategies.

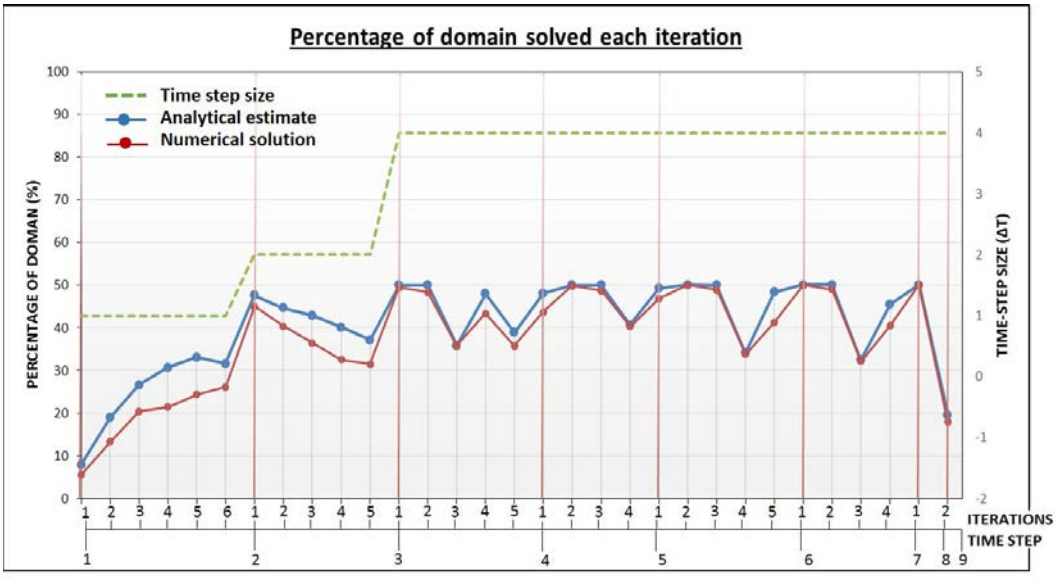

Figure 6: Percentage of domain solved over several time-steps for the arithmetic homogenization strategy applied on the SPE10 comparative study case.

8 Conclusions

An algorithmic approach and associated theory is developed to exploit the locality present in the nonlinear solution processes for flow in porous media. The methods are conservative and reproduce the Newton updates exactly, thereby preserving the nonlinear convergence rate. The degree of locality depends on the physics and complexity of the problem. It is a strong function of the compressibility of the system and the numerical time-step size. Advanced homogenization strategies can be developed to obtain conservative and sharp estimates such as the arithmetic averaging strategy. Gains of up to 95 fold were obtained for homogeneous simple problems. Up to 6 fold gains were observed in the computational time for the case of highly complex problems. The future work includes extending this algorithm to general fully-implicit simulation of coupled flow and multicomponent transport.

References

[1] K. Aziz and A. Settari. *Petroleum reservoir simulation*. Chapman & Hall, 1979.

[2] Z. Chen, G. Huan, and Y. Ma. *Computational methods for multiphase flows in porous media*, volume 2. Siam, 2006.

[3] W. Hundsdorfer and J.G. Verwer. *Numerical solution of time-dependent advection-diffusion-reaction equations*, volume 33. Springer Science & Business Media, 2013.

[4] G.J. McRae, W.R. Goodin, and J.H. Seinfeld. Numerical solution of the atmospheric diffusion equation for chemically reacting flows. *Journal of Computational Physics*, 45(1):1–42, 1982.

[5] G.I. Montecinos and E.F. Toro. Reformulations for general advection–diffusion–reaction equations and locally implicit ader schemes. *Journal of Computational Physics*, 275:415–442, 2014.

[6] D.W. Peaceman. *Fundamentals of numerical reservoir simulation*. Elsevier, 2000.

[7] T.H. Pulliam. Early development of implicit methods for computational fluid dynamics at nasa ames. *Computers & Fluids*, 38(3):491–495, 2009.

[8] T.F. Russell and M.F. Wheeler. Finite element and finite difference methods for continuous flows in porous media. *The mathematics of reservoir simulation*, 1:35–106, 1983.

[9] S.M. Sheth and R.M. Younis. Asynchronous multirate newton - a class of nonlinear solver that adaptively localizes computation. In *14th European conference on the mathematics of oil recovery*, 2014.

[10] S.M. Sheth and R.M. Younis. Localized linear systems for sequential implicit simulation of flow and transport. In *SPE Reservoir Simulation Symposium*. Society of Petroleum Engineers, 2015.

[11] J.G. Verwer, E.J. Spee, J.G. Blom, and W. Hundsdorfer. A second-order rosenbrock method applied to photochemical dispersion problems. *SIAM Journal on Scientific Computing*, 20(4):1456–1480, 1999.

[12] R.M. Younis. A sharp analytical bound on the spatiotemporal locality in general two-phase flow and transport phenomena. *Procedia Computer Science*, 18:473–480, 2013.